Ultrasensitive Detection of Cymbidium Mosaic Potexvirus Using a Single-Wall Carbon Nanotube-Functionalized Quartz Crystal Microbalance

2010 Jpn. J. Appl. Phys. 49 105103

(http://iopscience.iop.org/1347-4065/49/10R/105103)

Ultrasensitive Detection of Cymbidium Mosaic Potexvirus Using a Single-Wall Carbon Nanotube-Functionalized Quartz Crystal Microbalance

Yu-Shiun Chen[1,5], Yao-Ching Hung[2], Jin-Chern Chiou[3], Hui-Liang Wang[4], Hung-Shu Huang[1], Li-Chia Huang[2], and Guewha Steven Huang[1*]

[1]*Institute of Nanotechnology, Department of Materials Science and Engineering, National Chiao Tung University, 1001 University Road, EE137, Hsinchu 300, Taiwan, Republic of China*
[2]*Departments of Obstetrics and Gynecology, School of Medicine, China Medical University and Hospital, 91 Hsueh-Shih Road, Taichung 404, Taiwan, Republic of China*
[3]*Institute of Electrical Control Engineering, National Chiao Tung University, 1001 University Road, EE772, Hsinchu 300, Taiwan, Republic of China*
[4]*Department of Biotechnology, National Kaohsiung Normal University, 62 Shen Jhong Road, Kaohsiung 824, Taiwan, Republic of China*
[5]*Institute of Materials Science and Engineering, National Chiao Tung University, 1001 University Road, EE137, Hsinchu 300, Taiwan, Republic of China*

Received March 18, 2010; revised July 21, 2010; accepted August 8, 2010; published online October 20, 2010

We have developed an ultrasensitive, convenient, real-time platform for detecting Cymbidium mosaic potexvirus (CymMV) based on single-wall carbon nanotube (SWNT)-functionalized quartz crystal microbalance (QCM) sensors. Functionalization was achieved by coating the QCM electrode with SWNTs, followed by 1,1′-carbonyldiimidazole-activated Tween 20 (CDI–Tween 20) modification and conjugation of antibodies. Sensitivity was enhanced from 2.18 to 11.5 Hz ng^{-1} when 0.1 μg mL^{-1} CymMV was applied. The low limit of detection of SWNT-functionalized QCM sensors was improved from 2.08 to 0.502 ng. The SWNT-functionalized QCM sensor was successfully used to quantify the amount of CymMV contained in infected orchid leaves. Compared to enzyme-linked immunosorbent assay (ELISA), SWNT-functionalized QCM sensors are fast, economical, and ultra-sensitive, with comparable sensitivities. The current study demonstrates the application of QCM sensors as a convenient platform to detect and quantify CymMV.

DOI: 10.1143/JJAP.49.105103

1. Introduction

Cymbidium mosaic potexvirus (CymMV) and odontoglossum ringspot tobamovirus (ORSV) are the most prevalent and economically important viruses.[1–4] CymMV induces floral and foliar necrosis. ORSV causes ring spots on leaves and color breaking on flowers. Co-infections of both viruses cause blossom brown necrotic streak. The virus reduces plant vigor and flower quality, thus influencing the economic value.[5]

A number of methods have been developed to analyze CymMV, e.g., enzyme-linked immunosorbent assay (ELISA),[6,7] liquid chromatography–mass spectrometry (LC–MS) and matrix-assisted laser desorption-ionization (MALDI),[8] reverse transcription polymerase chain reaction (RT–PCR),[9] immuno-capillary zone electrophoresis (I-CZE),[10] and DIG-labeled cRNA probes.[11] Some of these methods require additional time-consuming labeling and amplification procedures. These methods are sensitive; however, they require hours and trained personnel to obtain unambiguous results.

A QCM is a mass detection device that operates based on the piezoelectric properties of quartz crystal.[12–15] QCMs are unsophisticated and cost-effective, have a real-time response and a high resolution, and are stable. Therefore, QCMs have been applied in recent years as biosensors for the real-time detection of liquid phase samples, such as protein, DNA, RNA, and heavy metal ion solutions.[16–19] QCMs have also been applied in the detection of CymMV, and provide the advantages of convenience and economy.[20] However, sensitivity and stability might be improved by further modification.

Fabrication of nanostructures on the interfaces of biosensors often leads to vast improvements, including significantly enhanced sensitivities with deposition of nanoparticles onto optical sensors[21] and surface plasmon resonance sensors,[22] nanowire-[23] and nanotube-[24] functionalization of field effect transistor (FET) sensors, and the use of other nano-scale sensors [25]. Surface modification of QCM electrodes is also performed using single-wall carbon nanotubes (SWNT).[25] However, enhancements in sensitivity and stability and application to field detection have yet to be demonstrated. The current study is based on SWNT-modified QCM sensors and applies to the detection of CymMV. SWNT-modified QCM sensors showed approximately a 1.5-fold increase in sensitivity over that of the control naked QCM sensors due to single-wall carbon nanotubes increasing the surface area of QCM sensors. The advantages using single-wall carbon nanotube are its excellent electrical conductivity, inertial chemical stability, and high affinity to CymMV that the limit of detection (LOD) can significantly lower.

Compared to traditional detection methods, our study provides a rapid, convenient, and economical method with a comparable sensitivity for quantification of the amount of CymMV in general orchid plants.

2. Experimental Procedure

2.1 QCM experiment

An oscillator (Catalog No. 35366-10) and a flow cell (Catalog No. 35363) were purchased from International Crystal Manufacturing. The QCM was fabricated from a 0.2-mm-thick AT-cut quartz wafer. A laboratory-constructed transistor–transistor logic integrated circuit (TTLIC) was used to power the QCM. An Agilent HP 53132 universal frequency counter was used to monitor the frequency output.

2.2 Fabrication of SWNT-functionalized QCM

A gold electrode was cleaned by immersing in 1.2 M NaOH for 20 min, 1.2 M HCl for 5 min, and distilled water for

*E-mail address: gstevehuang@mail.nctu.edu.tw

5 min. After a final rinse with 95% ethanol, it was air-dried at room temperature.

A typical SWNT film was formed on a quartz crystal surface by first dispersing bulk SWNTs (Sigma) produced by high-pressure CO in chloroform at a concentration of 50 μg mL^{-1}. One hundred microliters of this suspension was then deposited onto the crystal surface dropwise and baked at 60 °C for 1 h. Control experiments were done on bare QCM substrates without deposited nanotubes. The sample was examined with atomic force microscopy (AFM) for size and homogeneity.

2.3 Activation of CDI–Tween 20 for Conjugation to anti-CymMV

Five milligrams of Tween 20 (J. T. Baker) and 4.0 g 1,1-carbonyldiimidazole (CDI) (Fluka) were allowed to react in 25 mL dimethylsulfoxide (DMSO; Fluka, dried under a molecular sieve) at 40 °C for 2 h with stirring. Ethyl ether (J. T. Baker) was then added to cause precipitation, after which the precipitates were collected, dissolved in DMSO, and precipitated in ether. This process was repeated twice to ensure the removal of excess CDI, and was followed by drying the intermediate *in vacuo* overnight.[25] The CDI–Tween 20 composite was examined by fourier transform infrared spectroscopy (FTIR) spectrum 100. For conjugation to anti-CymMV antibodies, nanotube samples were first exposed to CDI–Tween 20 (1% w/v in water) for 30 min, and then rinsed thoroughly with water to remove excess reagents. The samples were then incubated in 1 μg mL^{-1} anti-CymMV in PBS buffer for 24 h and washed with PBS buffer for 1 min, then with deionized water. Raman spectroscopy was used to examine each step of modification. Additionally, the frequencies of all QCMs were monitored until steady state conditions were achieved (usually 30 min to 1 h), following which 20 μL of sample was injected.

2.4 ELISA

Each microwell of a 96-well Corning plate was pretreated with 100 μL 3% glutaraldehyde for 30 min at room temperature, followed by phosphate buffered saline (PBS) washing. One hundred microliters of properly diluted CymMV were added to the microwells and incubated for 2 h at room temperature, followed by Milli-Q water washing three times, and then washing with PBS three times. Blocking for nonspecific binding was performed by adding 100 μL of 3% BSA and incubating for 4 h at room temperature, followed by PBS washing three times.

Binding was performed by adding 100 μL properly diluted antiserum into the microwells and incubating for 1 h at room temperature, followed by thorough washes. Horseradish peroxidase (HRP)-conjugated anti-rabbit IgG, 2,2-azino-bis(3-ethylbenzthiazoline-6-sulfonic acid) (ABTS), and H_2O_2 were added in sequence to the wells according to the manufacturer's protocol, and the binding efficiency was monitored by absorbance at 405 nm.

2.5 CymMV purification and antisera production

CymMV was purified according to Wong and coworkers.[26] Fresh CymMV-infected leaves (100 g) were homogenized in a Waring blender (Waring Products) for 5 min with 500 mL of extraction buffer (0.1% β-mercaptoethanol, 0.01 M ethylenediaminetetraacetic acid (EDTA), and 0.1 M sodium phosphate buffer, pH 7.5). The extract was clarified with 100 mL of chloroform and centrifuged at 8,000 g for 10 min at 4 °C. The supernatant was filtered through cheesecloth before sodium chloride (NaCl) and poly(ethylene glycol) (PEG; molecular weight 8,000) were added to final concentrations of 0.25 and 4%, respectively. The mixture was centrifuged at 8,000 g for 20 min at 4 °C. The pellet was suspended in 5 mL of suspension buffer (1% Triton X-100 and 0.1 M sodium borate buffer, pH 8.0) and stirred slowly for 12 h at 4 °C. The suspension was centrifuged at low speed (8,000 g) to remove debris, and the supernatant was centrifuged at 90,000 g for 2.5 h at 4 °C. The pellet was suspended in 2 mL of 0.01 M sodium borate buffer, pH 7.5, and stored at −20 °C. The purified CymMVs were characterized by a scanning electron microscope (SEM) (Fig. 1). The CymMV particle lengths ranged from about 40 to 550 nm, with widths of approximately 15 nm. The scale bar is 100 nm. To generate infected plants, purified CymMV was injected into the leaves for 2 weeks. The sap was extracted from the diseased leaves (1 g) for detection.

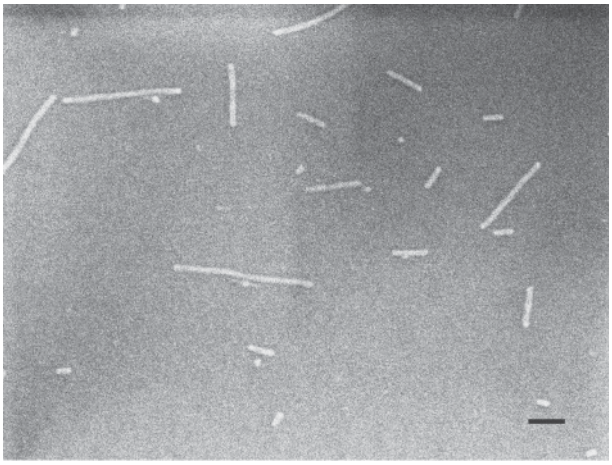

Fig. 1. SEM image of purified CymMV. The particle lengths ranged from about 40 to 550 nm, with widths of approximately 15 nm. The scale bar is 100 nm.

Purified CymMV (1 mg) was suspended in 1 mL of 0.02 M sodium phosphate buffer, pH 7.0, and emulsified with an equal volume of Freund's incomplete adjuvant (Sigma-Aldrich) by vortexing for 1 min. The resulting emulsion was injected intramuscularly into the hind legs of a New Zealand White rabbit. Booster injections of 1 mg each were administered 14, 21, and 28 days after the first injection. Before each booster injection, 10 mL of blood was drawn from the ear of the rabbit. The antiserum collected was divided into 1-mL aliquots and stored at 4 °C.

3. Results and Discussion

3.1 Fabrication of SWNT-functionalized QCM

Nonspecific binding to SWNTs was found to be a general phenomenon for all proteins examined in recent studies. This spontaneous adsorption onto carbon nanotubes has been attributed to hydrophobic interactions between the proteins and the nanotube surface.[27,28] In the current study, CDI–Tween 20 was conjugated to the side walls of SWNTs by hydrophobic interaction. The antibodies were crosslinked

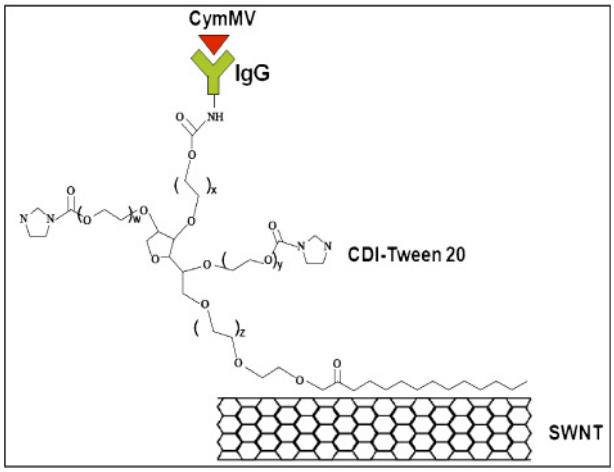

Fig. 2. (Color online) Schematic representation of functionalization with SWNT/CDI–Tween 20 on a QCM. CDI–Tween 20 was conjugated to the side walls of the SWNTs by hydrophobic interaction. The antibodies were crosslinked to the amine group of CDI–Tween 20 for virus detection.

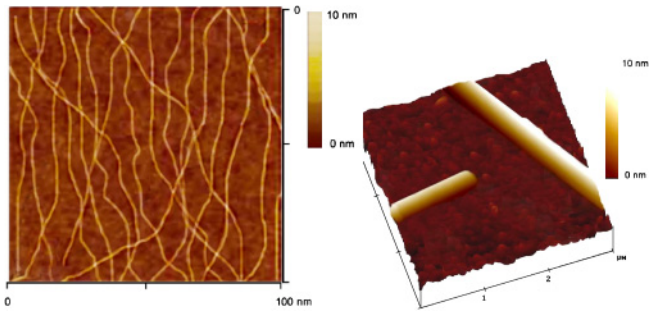

Fig. 3. (Color online) AFM image of the SWNT functionalized QCM. The SWNT length is about 1–2 μm and the diameter is 3–5 nm.

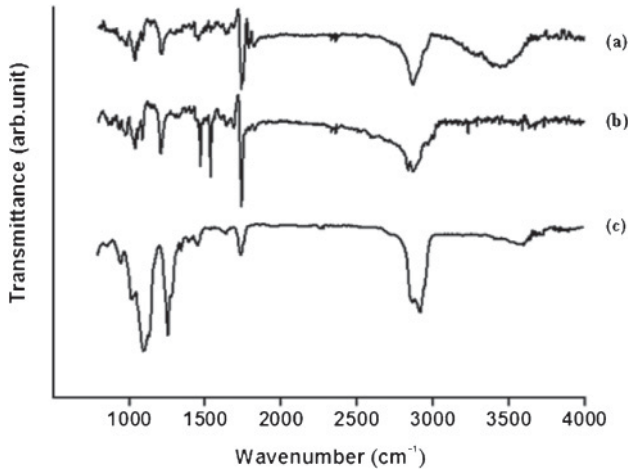

Fig. 4. FTIR spectra acquired from the CDI–Tween composite: (a) Tween 20, (b) CDI, and (c) CDI–Tween 20.

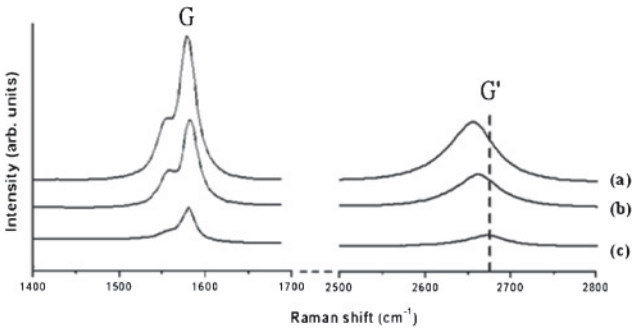

Fig. 5. Raman spectra of (a) purified SWNTs, (b) SWNTs functionalized with CDI–Tween 20, and (c) SWNT/CDI–Tween 20 conjugated to antibodies.

to the amine group of CDI–Tween 20 for virus detection (Fig. 2).

High-yield SWNTs were uniformly coated onto the gold electrode of the QCM. The diameter of the SWNTs was 3–5 nm and the length was 1–2 μm, as determined by an atomic force microscope (AFM) (Fig. 3). The SWNT surface was functionalized with CDI–Tween 20. Tween 20 contains functional groups similar to PEG and a long alkyl chain moiety. PEG moieties were crosslinked to CDI. The synthesis of the CDI–Tween 20 composite was examined by FTIR spectroscopy (Fig. 4). The spectrum of Tween 20 is characterized by an O–H band at 3440 cm^{-1}, a C–H band at 2870 cm^{-1}, and a C=O band at 1742 cm^{-1} [Fig. 4(a)]. The spectrum of CDI contains a C–H band at 2870 cm^{-1}, a C=O band 1742 cm^{-1}, a C–N band at 1050 cm^{-1}, and a C=N band at 1538 cm^{-1} [Fig. 4(b)]. The CDI–Tween 20 conjugate spectrum showed a C–H band at 2924 cm^{-1}, a C–N band at 1744 cm^{-1}, and a C–O band at 1107 cm^{-1} [Fig. 4(c)]. The result demonstrated that the PEG structures were converted to amine groups, as indicated by the disappearance of the O–H peak.

Raman spectra were used to monitor the step-by-step chemical fabrication (Fig. 5). The unique properties of SWNTs arise from their particular one-dimensional structure, which is directly linked to the characteristic Raman bands (G band). The adsorption of SWNTs onto QCMs was characterized by an enhanced G band at 1581 cm^{-1} that dominated the spectra and was significantly stronger than the G′ band at 2659 cm^{-1} [Fig. 5(a)]. The functionalization of CDI–Tween 20 to SWNT shifted the G′ band to 2664 cm^{-1}, whilethe G band remained at 1581 cm^{-1} [Fig. 5(b)]. The conjugation of the anti-CymMV antibody to CDI–Tween 20/SWNT shifted the G′ band to 2675 cm^{-1}, whereas the G band remained at 1581 cm^{-1} [Fig. 5(c)]. The frequency shift of the G′ band indicated an increase in size of the SWNTs due to the functionalization with CDI–Tween 20.[29)]

The functionalization of the SWNTs improved the mechanical and electrical properties. Nonspecific binding of SWNTs was blocked by the conjugated CDI–Tween 20 copolymer chains, thus enhancing the specificity during bio-detection.

3.2 Detection of CymMV using SWNT-functionalized QCM

The SWNT-functionalized QCM sensors were used for the detection of purified CymMV. The control experiment was performed by immobilizing anti-CymMV antibodies on the naked QCM electrode. Twenty microliters of CymMV at various concentrations were injected into the QCM–FIA system, and the resonant frequency was monitored in real time (Fig. 6). A 5-fold enhancement in sensitivity was observed at 2.08 ng CymMV, from 2.18 to 11.56 Hz ng^{-1}

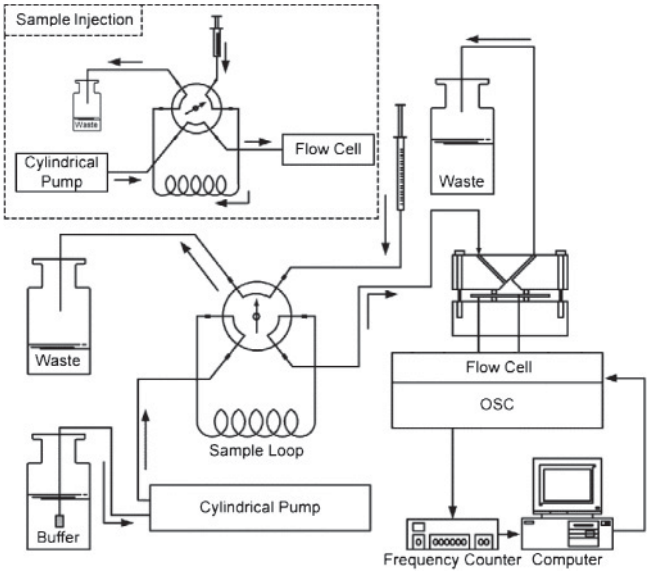

Fig. 6. Scheme for the QCM flow injection analysis apparatus. Continuous flow was achieved using a cylindrical pump. The sample was injected through an injection loop and pumped into the flow cell.

Table I. Comparison of the sensitivities of naked QCMs and SWNT-functionalized QCMs.

CymMV ($\mu g\,mL^{-1}$)	Sensitivity[a] ($Hz\,ng^{-1}$)	
	Naked	SWNT/CDI–Tween 20
1.034	3.05	4.55
0.517	4.64	7.13
0.258	2.42	8.08
0.103	2.18	11.5
0.052	2.61	9.89
0.026	1.68	8.22
0.013	3.05	4.54
0.010	4.64	7.13

a) Sensitivity is defined as the change in frequency shift per applied virus weight. The injection volume is 20 μL. Sensitivity (S) = $\Delta F/\Delta m$. ΔF: frequency shift; Δm: applied weight.

(Table I). The limit of detection (LOD) is defined as three times the standard deviation of the background noise (S/N > 3, noise ~0.78 Hz). The LODs of the control experiment and the SWNT functionalization experiment were 2 ng (10^{-4} mg mL^{-1}) and 0.5 ng (2.5×10^{-5} mg mL^{-1}) and the signals were 4.5 and 4.25 Hz, respectively (Fig. 7).

Immuno-detection by ELISA is the most popular method for CymMV detection. The purified CymMV was therefore also examined by ELISA (Fig. 8). The LOD of ELISA was 0.13 ng (1.29×10^{-6} mg mL^{-1}, 100 μL per well). The sensitivity and LOD of the functionalized QCM sensors were comparable to ELISA.

Our platform was also successfully used for field detection of CymMV using infected orchid leaves. The detection of CymMV was performed for 11 orchids (including 10 infected plants and 1 healthy plant) using the SWNT-functionalized QCM sensor. The amount of virus per gram of leaves was between 11.5–40.2 μg viruses per gram of leaves (Fig. 9). The uninfected orchid showed negative results in the detection.

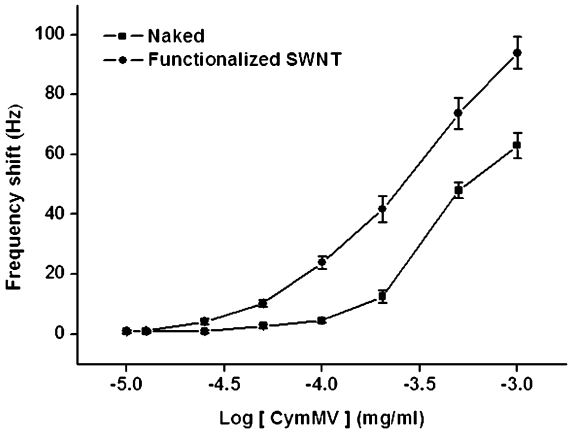

Fig. 7. Injection of purified CymMV into the IgG-coated QCM sensor. The QCM electrode was coated with IgG antiserum by naked SWNTs and SWNTs functionalized with CDI–Tween 20. The frequency shift was measured after injection of 20 μL of purified CymMV.

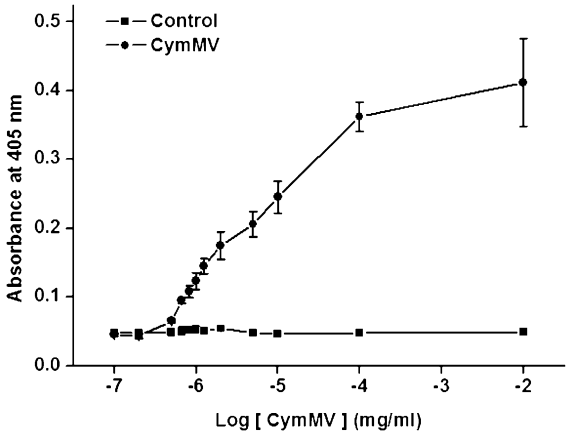

Fig. 8. ELISA characterization of purified virus at various concentrations.

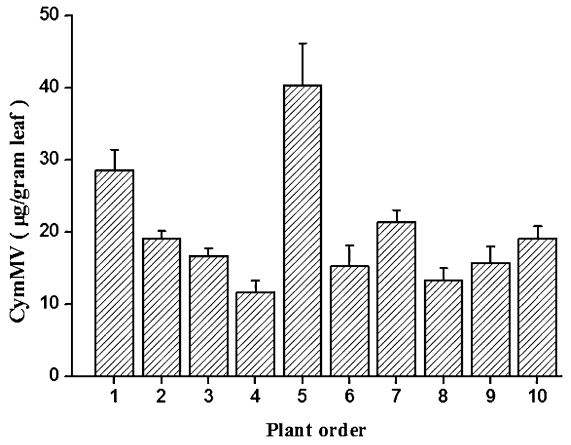

Fig. 9. Quantification of the amount of CymMV per gram of leaves. The quantity of CymMV was calculated using a purified CymMV standard curve.

4. Conclusions

We have developed an ultra-sensitive, convenient real-time platform for detecting CymMV based on SWNT-functionalized QCM sensors. Sensitivity was enhanced from 2.18 to

11.5 Hz ng^{-1} when 0.1 μg mL^{-1} CymMV was applied. The low limit of detection of SWNT-functionalized QCM sensors was improved from 2.08 to 0.502 ng. The SWNT-functionalized QCM sensor was successfully used to quantify the amount of CymMV in infected orchid leaves. Compared to ELISA, SWNT-functionalized QCM sensors are fast, economical and ultra-sensitive, with comparable sensitivity. The current study demonstrates that QCMs are a convenient platform for the detection and quantification of CymMV.

Acknowledgements

This study was supported in part by the National Science Council in Taiwan (grants NSC99-2320-B-039-015-MY3, NSC97-2923-B-009-001-MY3, and NSC 97-2320-B-009-002-MY3) and the Bureau of Animal and Plant Health Inspection and Quarantine Council of Agriculture in Taiwan (Grant 98AS-9.2.4-BQ-B1).

1) F. W. Zettler, N. J. Ko, G. C. Wisler, M. S. Elliott, and S. M. Wong: Plant Disease **74** (1990) 621.
2) S. Wong, C. Chng, Y. Lee, K. Tan, and F. Zettler: Crop Prot. **13** (1994) 235.
3) K. Ryu, W. Park, S. Chung, and K. Yoon: Plant Disease **79** (1995) 321.
4) M. Moles, H. Delatte, K. Farreyrol, and M. Grisoni: Arch. Virol. **152** (2007) 705.
5) M. N. Pearson and J. S. Cole: J. Phytopathol. **131** (1991) 193.
6) R. Vejaratpimol, C. Channuntapipat, P. Liewsaree, T. Pewnim, K. Ito, M. Iizuka, and N. Minamiura: J. Ferment. Bioeng. **86** (1998) 65.
7) M. Grisoni, F. Davidson, C. Hyrondelle, K. Farreyrol, M. Caruana, and M. Pearson: Plant Disease **88** (2004) 119.
8) S. W. Tan, S. M. Wong, and R. M. Kini: J. Virol. Methods **85** (2000) 93.
9) A. J. C. Eun, M. L. Seoh, and S. M. Wong: J. Virol. Methods **87** (2000) 151.
10) A. Eun and S. Wong: Phytopathology **89** (1999) 522.
11) W. W. Hu and S. M. Wong: J. Virol. Methods **70** (1998) 193.
12) D. Buttry and M. Ward: Chem. Rev. **92** (1992) 1355.
13) J. Rickert, A. Brecht, and W. Gopel: Anal. Chem. **69** (1997) 1441.
14) W. W. Hu, S. M. Wong, C. J. Goh, and C. S. Loh: Arch. Virol. **143** (1998) 1265.
15) G. S. Huang, M. T. Wang, and M. Y. Hong: Analyst **131** (2006) 382.
16) G. S. Huang, M. T. Wang, C. W. Su, Y. S. Chen, and M. Y. Hong: Biosens. Bioelectron. **23** (2007) 319.
17) M. Lazerges, H. Perrot, N. Zeghib, E. Antoine, and C. Compere: Sens. Actuators B **120** (2006) 329.
18) Y. Liu, X. Yu, R. Zhao, D. H. Shangguan, Z. Y. Bo, and G. Q. Liu: Biosens. Bioelectron. **19** (2003) 9.
19) L. Tedeschi, L. Citti, and C. Domenici: Biosens. Bioelectron. **20** (2005) 2376.
20) A. J. Eun, L. Huang, F. T. Chew, S. F. Li, and S. M. Wong: J. Virol. Methods **99** (2002) 71.
21) A. McFarland and R. Van Duyne: Nano Lett. **3** (2003) 1057.
22) A. Serra, E. Filippo, M. Re, M. Palmisano, M. Vittori-Antisari, A. Buccolieri, and D. Manno: Nanotechnology **20** (2009) 165501.
23) F. Patolsky, G. F. Zheng, O. Hayden, M. Lakadamyali, X. W. Zhuang, and C. M. Lieber: Proc. Natl. Acad. Sci. U.S.A. **101** (2004) 14017.
24) T. Someya, J. Small, P. Kim, C. Nuckolls, and J. Yardley: Nano Lett. **3** (2003) 877.
25) R. Chen, S. Bangsaruntip, K. A. Drouvalakis, N. W. S. Kam, M. Shim, Y. Li, W. Kim, P. J. Utz, and H. Dai: Pro. Natl. Acad. Sci. U.S.A. **100** (2003) 4984.
26) S. M. Wong, P. H. Mahtani, K. C. Lee, H. H. Yu, Y. Tan, K. K. Neo, Y. Chan, M. Wu, and C. G. Chng: Arch. Virol. **142** (1997) 383.
27) M. Shim, N. Kam, R. Chen, Y. Li, and H. Dai: Nano Lett. **2** (2002) 285.
28) R. Chen, Y. Zhang, D. Wang, and H. Dai: J. Am. Chem. Soc. **123** (2001) 3838.
29) A. Hartschuh, E. Sánchez, X. Xie, and L. Novotny: Phys. Rev. Lett. **90** (2003) 095503.